Available online at www.sciencedirect.com

ScienceDirect

Journal of the Franklin Institute 360 (2023) 8550–8568

www.elsevier.com/locate/jfranklin

# Stabilization for a class of strict-feedback nonlinear systems via the PWM control law

Le Chang, Xiaowei Shao*, Dexin Zhang

*School of Aeronautics and Astronautics, Shanghai Jiao Tong University, Shanghai, 200240, China*

Received 21 December 2022; received in revised form 5 May 2023; accepted 16 June 2023
Available online 22 June 2023

**Abstract**

This paper studies the PWM control problem of a class of nonlinear systems. During a modulation period, the PWM control signal maintains a pulse waveform with tunable width and fixed magnitude. The PWM control only possesses finite states, and has relatively limited control capability. This causes the degradation of system performance, and even the instability when implementing into a nonlinear system. We will introduce a novel method to design both the state feedback stabilizer and the output feedback stabilizer for strict-feedback nonlinear systems via the PWM control. The system performance is analyzed in a novel framework and the stability criteria is derived to ensure the system convergence. At last, two examples are considered to illustrate the effectiveness of our proposed method.


## 1. Introduction

Designing the stabilizing controller plays a crucial role in the study of control systems [1]. The advent of computer-based and digitally networked control systems requires the analogue plant outputs and the control variables be finite bit-strings or discrete symbols for storage, manipulation and transmission [2]. This process of converting a continuous-valued variable into a finite-valued one entails a potentially significant loss of resolution. The system performance is unavoidable to be degraded, even results in the system instability. Thus, it is desired to stabilize the system by studying the digital controller.

* Corresponding author.
*E-mail addresses:* le@lchang.me (L. Chang), shaoxwmail@163.com (X. Shao), dx_zhang@sjtu.edu.cn (D. Zhang).

https://doi.org/10.1016/j.jfranklin.2023.06.027
0016-0032/

The nonlinear phenomena are unavoidable in nature, and many results has been reporting the related algorithms on nonlinear systems [3,4]. The strict-feedback nonlinear system belongs to an important class of nonlinear systems. There are three main approaches to design the control for this system. One is the backstepping method, where the control input is achieved based on a series of auxiliary input. A detailed design process was introduced in [5], and some recent develop results could be seen in [6–10]. Another design technology is based on high gain feedback control, where the control is characterized by a parameter and this parameter is determined through analyzing the system nonlinear terms. It was widely considered in [11–14] to design the stabilizing or regulating controller for strict-feedback nonlinear systems. The last is the intelligent control, where the fuzzy technologies or the neural technologies are utilized to approximate the system nonlinear terms. For example, based on the fuzzy approximate approach, [15] combined the high-gain observer and the adaptive design method to solve the tracking problem for the strict-feedback nonlinear systems. [16] employed the neural network to approximate the uncertain nonlinear dynamics and developed the backstepping method to give the tracking controller. In [17], after using fuzzy logic systems (FLSs) to estimate the unknown nonlinear functions, the backstepping method was applied to the design of adaptive fuzzy controller. However, the designed controllers in above results have a continuous form, and the performance of digitization is needed to be further analyzed.

There are some existing results focusing on the digitizing controller problem for the strict-feedback nonlinear systems. One point is considering the sampled-data control. In this case, the analogue outputs or states are measured at the sampling instants, and then the designed control signal is holding during a period. For example, [18] studied the sampled-data output stabilization problem for the strict-feedback nonlinear systems based on the high gain feedback control method. For the large-scale systems, [19] designed the tracking controller when the interconnections between subsystems were unknown. Another point is considering the quantized control. The process of quantized signal is to map an infinite set of continuous values into a finite set of quantized values. For nonlinear system, some design problems of quantized controller were solved in [20–22]. Specially, [23] gave a quantized controller for the strict-feedback nonlinear systems when the nonlinear terms were unknown. But, it is noted that the control input generated by the sampling and the quantizing has infinite states.

The pulse width modulation(PWM) can be seen as a kind of quantized scheme. It converts the signal into two or three levels, which corresponds to the ON-OFF switching of the actuator (or controller) [24]. Such an ON-OFF characteristic is also beneficial to encode desired continuous-time information into digital bits, which aligns with nowadays wireless communication paradigms. In the context of PWM control, the time is partitioned into a series of equal cycles, and then the PWM control signal turns the actuator ON over a portion of each cycle and switches it OFF during the rest of the cycle. However, it should be pointed out that the ON-OFF switching actuator (or controller) introduces strong nonlinear characteristics such as discontinuity and saturation to the system. It is for this reason that a direct implementation of PWM control may not yield satisfactory performance. Much research effort has therefore been devoted to determining the PWM duty cycle fulfilling the required system performance [25–27]. So far, several attractive methods have been developed in the past few years, such as sliding mode control [28,29], hybrid control [30,31], and LQ optimal control [32,33]. Nevertheless, it is noteworthy that the inherent nonlinearity of the physical systems concerned in these studies is unfortunately neglected, which implies that the desired control performance may not be preserved in realistic scenarios as most practical control systems are complexly

nonlinear. As a result, the following two essential challenging issues are identified for achieving the PWM controller design of strict-feedback nonlinear systems: 1) how to ensure that the finite level states could stabilize the strict-feedback nonlinear system? and 2) how to cope with both the inherent nonlinearity of systems and the nonlinear character of PWM signal? To the best of our knowledge, the above two issues remain challenging in the PWM control literature, which motivates this study.

In this paper, we develop a novel PWM controller design method that provides feasible solutions to the above two questions. The specific features are summarized as follows. *1) The strict-feedback nonlinear system is stabilized through a PWM signal involving three states*. Different from the continuous-time controller [14–16], the sampled-and-hold controller [18,34], and the quantized controller [35,36], we present a novel method to design the stabilizing controller which only switches between three states $-m$, $-1$, and $m$. Although the PWM signal can approximate the continuous-time signal with a small sampling size, the approximating error still exists and degrades the system performance. *2) A novel stable analyzing method is presented to ensure the convergence of the generated closed-loop system.* Inspired by [37,38] which considered the hybrid observer, we extended the results to study the PWM control due to the impulse character. Through establishing a new relation for matrices, the convergence of the generated closed-loop system is guaranteed.

The remainder of this paper is structured as follows. We will describe the problem in Section 2. The state feedback controller will be designed in Section 3, while the output feedback controller will be discussed in Section 4. Two examples will be present in Section 5 to illustrate the main results. Some ending remarks will be summarized in Section 6, while a reference list will end this paper.

*Notation:* We employ $\|\cdot\|$ to denote the Euclidean norm for vectors, or the induced Euclidean norm for matrices. We use $I$ to denote an $n \times n$ identity matrix. $\text{sign}(\cdot)$ is the signum function defined as: $\text{sign}(x) = -1$ if $x < 0$, $\text{sign}(x) = 0$ if $x = 0$, and $\text{sign}(x) = 1$ if $x > 0$.

## 2. Problem formulation

The strict-feedback nonlinear system addressed in the paper is

$$\begin{aligned}
\dot{x}_i(t) &= x_{i+1}(t) + f_i(x_1(t), x_2(t), \ldots, x_i(t)), \quad i = 1, 2, \ldots, n-1 \\
\dot{x}_n(t) &= u(t) + f_n(x_1(t), x_2(t), \ldots, x_n(t)), \\
y(t) &= x_1(t),
\end{aligned} \tag{1}$$

where $x_i$ is $i$th element of system state $x = (x_1, x_2, \ldots, x_n)^T \in \mathbb{R}^n$, $u \in \mathbb{R}$ is the system input, $y \in \mathbb{R}$ is the system output. The initial instant $t_0$ is assumed as 0, and the initial state is $x(t_0) \in \mathbb{R}^n$. The nonlinear function $f_i$ $(i = 1, 2, \ldots, n)$ is continuous and satisfies the following assumption.

**Assumption 1.** For any $x_1, x_2, \ldots, x_n \in \mathbb{R}$, it holds that

$$|f_i(x_1, x_2, \ldots, x_i)| \le \theta(|x_1| + |x_2| + \ldots + |x_i|), \quad i = 1, 2, \ldots, n, \tag{2}$$

where $\theta$ is a positive constant.

**Remark 1.** System (1) under Assumption 1 is called the strict-feedback nonlinear system. Many existing results have been reporting on the control design for such nonlinear systems. For example, the output feedback control [12,15] designed the controller which is a continuous

signal; the sampled-data controller and the event-triggered controller was respectively designed in [18,34,38,39]; the quantized controller was given in [36]. Noticed that the values of all the above designed controllers were infinite. The problem is unsolved, as far as we know, that using finite values to stabilize the strict-feedback nonlinear system. This motivates this work.

The system state/output is measured at the instants $t_k = kT$ with $T > 0$ being the sampling size, and $k = 0, 1, 2, \ldots,$ being the sampling index. We propose the following three-level-state-dependent PWM control law to stabilize the system (1):

$$u(t) = \begin{cases} ms_k, & t \in [t_k, t_k + \delta_k), \\ 0, & t \in [t_k + \delta_k, t_{k+1}), \end{cases} \tag{3}$$

where $m$ is a prescribed positive constant representing the *amplitude* of the PWM signal, $s_k \in \{-1, 1\}$ represents the *sign* of the pulse during the $k$th sampling period, and $\delta_k$ is known as the *pulse width* during the $k$th sampling period. To make the PWM signal well-defined, it is required that $0 \le \delta_k \le T$. Then, the *duty cycle* of the PWM is defined as

$$d_k = \frac{\delta_k}{T} \cdot 100\% \in [0\%, 100\%] \tag{4}$$

which describes the proportion of on time to the regular interval $T$. In particular, when the control is off during $k$th sampling period, it has a duty cycle of $d_k = 0\%$. A low duty cycle corresponds to a low power of the control because the power is off for most of the time. Since the PWM control has only three states, it has relatively limited control capability.

It can be seen from (3) that the PWM control signal $u(t)$ is determined by two variables $d_k$ and $s_k$. Therefore, *the main objective of this work* is to design the two controller variables $d_k$, $s_k$ to achieve the stabilizing controller. Specifically, we consider the following two aspects:

- *Designing the state feedback controller:* Based on the measured state $x(t_k)$, proposing the PWM controller (3) such that the resulting closed-loop system is asymptotically stable at the equilibrium point $x = 0$.
- *Designing the output feedback controller:* Based on the measured output $y(t_k)$, designing the auxiliary variable $\hat{x}(t)$ and the PWM controller (3) such that the resulting closed-loop system is asymptotically stable at the equilibrium point $x = 0$, $\hat{x} = 0$.

## 3. State feedback control

### 3.1. Control design

The design of PWM control signal is mainly to determine the sign $s_k$ and the duty cycle $d_k$. In order to design these values, we introduce the auxiliary variables

$$z_1(t) = \frac{1}{r}x_1(t), \quad z_2(t) = \frac{1}{r^2}x_2(t), \quad \ldots, \quad z_n(t) = \frac{1}{r^n}x_n(t), \tag{5}$$

where $r \ge 1$ is a parameter to be designed.

By denoting $z = (z_1, z_2, \ldots, z_n)^T$, we design

$$s_k = \operatorname{sign}(Kz(t_k)), \quad d_k = \left| \frac{r^{n+1}Kz(t_k)}{m} \right| \cdot 100\%, \tag{6}$$

where $K = (k_1, k_2, \ldots, k_n)^T$ with $k_1$ to $k_n$ be the coefficients of a Hurwitz polynomial $p(s) = s^n + k_n s^{n-1} + \ldots + k_1$.

From (6), to ensure $d_k \leq 1$, we need a sufficient large amplitude $m$. It is reasonable to consider such a constant $m$. The strict-feedback nonlinear system is in complex form, and the control need a certain power. Then, the following relation is holding:

$$ms_k = \frac{r^{n+1} K z(t_k)}{d_k}. \tag{7}$$

### 3.2. Stability analysis

**Theorem 1.** *Supposed that Assumption 1 is satisfied. For any initial state $x(t_0) \in \mathbb{R}^n$, through choosing appropriate sampling size $T$ and control parameter $r$, system (1) can be stabilized through the PWM signal (3), (6) if the PWM amplitude $m$ is sufficient large.*

**Proof.** For the auxiliary variables $z = (z_1, z_2, \ldots, z_n)^T$, we obtain

$$\dot{z}(t) = rAz(t) + \frac{1}{r^n} Bu(t) + F(t), \tag{8}$$

where

$$A = \begin{pmatrix} 0 & 1 & 0 & \cdots & 0 \\ 0 & 0 & 1 & \cdots & 0 \\ \vdots & \vdots & \vdots & & \vdots \\ 0 & 0 & 0 & \cdots & 1 \\ 0 & 0 & 0 & \cdots & 0 \end{pmatrix}, B = \begin{pmatrix} 0 \\ 0 \\ \vdots \\ 0 \\ 1 \end{pmatrix}, F(t) = \begin{pmatrix} \frac{1}{r} f_1(x_1(t)) \\ \frac{1}{r^2} f_2(x_1(t), x_2(t)) \\ \vdots \\ \frac{1}{r^{n-1}} f_{n-1}(x_1(t), \ldots, x_{n-1}(t)) \\ \frac{1}{r^n} f_n(x_1(t), \ldots, x_{n-1}(t), x_n(t)) \end{pmatrix}. \tag{9}$$

Solving the above equation get

$$z(t_{k+1}) = e^{rTA} z(t_k) + \int_{t_k}^{t_{k+1}} e^{rA(t_{k+1}-s)} \frac{1}{r^n} Bu(s) ds + \int_{t_k}^{t_{k+1}} e^{rA(t_{k+1}-s)} F(s) ds. \tag{10}$$

Substituting the input (3), (6) into the above equation, we express the second item as

$$\begin{aligned} &\int_{t_k}^{t_{k+1}} e^{rA(t_{k+1}-s)} \frac{1}{r^n} Bu(s) ds = \int_0^{rT} e^{A(rT-s)} \frac{1}{r^{n+1}} Bu\left(t_k + \frac{s}{r}\right) ds \\ &= \int_0^{r\delta_k} e^{A(rT-s)} BKz(t_k) ds = \int_0^{r\delta_k} e^{A(rT-s)} \frac{1}{r^{n+1}} Bms_k ds \\ &= \frac{1}{d_k} \int_0^{rd_kT} e^{A(rT-s)} BKz(t_k) ds. \end{aligned} \tag{11}$$

Let

$$M(\alpha, \tau) = \left( e^{\alpha A} + \frac{1}{\tau} \int_0^{\tau\alpha} e^{A(\alpha-s)} BK ds \right) \tag{12}$$

be a matrix function defined on $[0, 1] \times (0, 1]$.

From (10), we get the closed-loop system as

$$z(t_{k+1}) = M(rT, d_k) z(t_k) + \tilde{F}(t_k), \tag{13}$$

where $\tilde{F}(t_k) = \int_{t_k}^{t_{k+1}} e^{rA(t_{k+1}-s)} F(s) ds$.

Noted that the choice of $K$ can make the matrix $A+BK$ be Hurwitz. A positive definite matrix $P$ can be found to meet

$$(A+BK)^T P + P(A+BK) \le -I. \tag{14}$$

Let the Lyapunov function be $V_k = z^T(t_k)Pz(t_k)$. Then, it holds

$$\begin{aligned} V_{k+1} &= \Big(M(rT,d_k)z(t_k) + \tilde{F}(t_k)\Big)^T P\Big(M(rT,d_k)z(t_k) + \tilde{F}(t_k)\Big) \\ &= z^T(t_k)M^T(rT,d_k)PM(rT,d_k)z(t_k) \\ &\quad +2z^T(t_k)M^T(rT,d_k)P\tilde{F}(t_k) + \tilde{F}^T(t_k)P\tilde{F}(t_k). \end{aligned} \tag{15}$$

To continue, we need to analyze the matrix function $M(\alpha,\tau)$ and the nonlinear function $\tilde{F}(t_k)$. On the one hand, the derivative of $M(\alpha,\tau)$ satisfies

$$\frac{\partial M(\alpha,\tau)}{\partial \alpha} = Ae^{\alpha A} + \frac{1}{\tau}A\int_0^{\tau\alpha} e^{A(\alpha-s)}BKds + e^{A(\alpha-\tau\alpha)}BK, \tag{16}$$

and

$$\frac{\partial^2 M(\alpha,\tau)}{\partial \alpha^2} = A^2e^{\alpha A} + \frac{1}{\tau}A^2\int_0^{\tau\alpha} e^{A(\alpha-s)}BKds + Ae^{A(\alpha-\tau\alpha)}BK + A(1-\tau)e^{A(1-\tau)\alpha}BK. \tag{17}$$

Considering the function

$$\omega(\alpha,\tau,v) = v^T M^T(\alpha,\tau)PM(\alpha,\tau)v, \quad \forall v \in \{v \mid \|v\| = 1\}, \tag{18}$$

we get

$$\omega(\alpha,\tau,v) = \omega(0,\tau,v) + \alpha\left.\frac{d\omega(\alpha,\tau,v)}{d\alpha}\right|_{\alpha=0} + \alpha^2\left.\frac{d^2\omega(\alpha,\tau,v)}{d\alpha^2}\right|_{\alpha=\xi}, \tag{19}$$

where $\xi \in [0,1]$.

On the other hand, due to $A^n = 0$, it holds

$$\begin{aligned} \frac{1}{\tau}\int_0^{\alpha\tau} e^{A(\alpha-s)}BKds &= \sum_{j=0}^{n}\frac{1}{(j+1)!}A^jBK\alpha^{j+1}\frac{1}{\tau}\big(1-(1-\tau)^{j+1}\big) \\ &= \sum_{j=0}^{n}\frac{1}{(j+1)!}A^jBK\alpha^{j+1}\big(1+(1-\tau)+\ldots+(1-\tau)^j\big). \end{aligned} \tag{20}$$

We get that $M(\alpha,\tau)$, $\partial M(\alpha,\tau)/\partial\alpha$ and $\partial^2 M(\alpha,\tau)/\partial\alpha^2$ are bounded.

Then, a constant $\alpha_m$ can be found such that

$$\omega(\alpha,\tau,v) \le \omega(0,\tau,v) - \frac{1}{2}\alpha v^T v, \quad \alpha \in [0,\alpha_m] \tag{21}$$

where $\partial M(\alpha,\tau)/\partial\alpha|_{\alpha=0} = -v^T v$ is utilized.

Since $v$ is arbitrarily chosen in $\{v \mid \|v\| = 1\}$, one obtains

$$M^T(\alpha,\tau)PM(\alpha,\tau) \le P - \frac{\alpha}{2}I, \quad \alpha \in [0,\alpha_m], \quad \tau \in [0,1]. \tag{22}$$

Back to (50), we turn to estimate the nonlinear term $\tilde{F}(t_k)$. Under Assumption 1, we get

$$\frac{1}{r^i}|f_i(x_1,x_2,\ldots,x_i)| \le \theta(|z_1|+|z_2|+\ldots+|z_i|) \le \theta\sqrt{n}\|z\|, \quad i = 1,2,\ldots,n, \tag{23}$$

which further yields

$$\|F(t)\| \le \theta n \|z\|. \tag{24}$$

Meanwhile, it holds

$$\frac{d}{dt}\|z(t)\| \le \|\dot{z}(t)\| \le r\|A\|\|z(t)\| + \frac{1}{r^n}\|B\||u(t)| + \theta n\|z(t)\|, \tag{25}$$

and

$$\int_{t_k}^{t_k+d_k} |u(s)|ds = |rKz(t_k)| \le r\|K\|\|z(t_k)\|. \tag{26}$$

In (25), integrating the left part from $t_k$ to $t$ $(t \in [t_k, t_{k+1}))$, one gets

$$\|z(t)\| \le \|z(t_k)\| + (r\|A\| + \theta n)\int_{t_k}^{t} \|z(s)\|ds + \|B\|\|K\|\|z(t_k)\|. \tag{27}$$

Then, using the Grönwall's inequality, one obtains

$$\|z(t)\| \le (1 + \|B\|\|K\|)e^{(r\|A\|+\theta n)(t-t_k)}\|z(t_k)\|. \tag{28}$$

In this case, the nonlinear term $\tilde{F}(t_k)$ is estimated as below:

$$\begin{aligned}
\left\|\tilde{F}(t_k)\right\| &\le \int_{t_k}^{t_{k+1}} e^{r\|A\|(t_{k+1}-s)}\|F(s)\|ds \\
&\le \int_{t_k}^{t_{k+1}} \theta n e^{r\|A\|(t_{k+1}-s)}(1 + \|B\|\|K\|)e^{(r\|A\|+\theta n)(s-t_k)}\|z(t_k)\|ds \\
&\le \int_{t_k}^{t_{k+1}} \theta n e^{rT\|A\|}(1 + \|B\|\|K\|)e^{\theta n(s-t_k)}\|z(t_k)\|ds \\
&\le e^{\|A\|}(1 + \|B\|\|K\|)\left(e^{\theta nT} - 1\right)\|z(t_k)\|.
\end{aligned} \tag{29}$$

Thus, back to (50), we get that, when $rT \le \alpha_m$, it holds

$$\begin{aligned}
V_{k+1} &\le V_k - \frac{rT}{2}\|z(t_k)\|^2 + 2z^T(t_k)M^T(rT, d_k)P\tilde{F}(t_k) + \tilde{F}^T(t_k)P\tilde{F}(t_k) \\
&\le V_k - \frac{rT}{2}\|z(t_k)\|^2 + 2\varpi\|P\|(1 + \|B\|\|K\|)e^{\|A\|}\left(e^{\theta nT} - 1\right)\|z(t_k)\|^2 \\
&\quad + \|P\|(1 + \|B\|\|K\|)^2 e^{2\|A\|}\left(e^{\theta nT} - 1\right)^2\|z(t_k)\|,
\end{aligned} \tag{30}$$

where $\varpi$ is the upper bounded of $\|M(\alpha, \tau)\|$ on the area $[0, 1] \times (0, 1]$.

When $T \in (0, 1]$, it holds

$$e^{\theta nT} - 1 \le T\left(e^{\theta n} - 1\right). \tag{31}$$

Thus, when

$$r \ge 8\varpi\|P\|(1 + \|B\|\|K\|)e^{\|A\|}\left(e^{\theta n} - 1\right) + 4\|P\|(1 + \|B\|\|K\|)^2 e^{2\|A\|}\left(e^{\theta n} - 1\right)^2, \tag{32}$$

we get

$$V_{k+1} \le V_k - \frac{rT}{4}\|z(t_k)\|^2. \tag{33}$$

This indicates the convergence of $V_k$. Since $r$ is a constant, it is easy to conclude that system (1) under PWM control (3), (6) is stable at equilibrium point $x = 0$.

The last work is to discuss the choosing of $m$.

It is needed that $m \geq |r^{n+1}Kz(t_k)|$ for any index $k$. Since

$$V_{k+1} \leq V_k \leq \ldots \leq V_0 \tag{34}$$

we get

$$\begin{aligned}&\left|r^{n+1}Kz(t_k)\right| \leq r^{n+1}\|K\|\|z(t_k)\| \leq r^{n+1}\|K\|\sqrt{\frac{V_k}{\lambda_{\min}(P)}} \leq r^{n+1}\|K\|\sqrt{\frac{V_0}{\lambda_{\min}(P)}}\\ &\leq r^{n+1}\|K\|\sqrt{\frac{\lambda_{\max}(P)}{\lambda_{\min}(P)}}\|z(t_0)\| \leq r^{n}\|K\|\sqrt{\frac{\lambda_{\max}(P)}{\lambda_{\min}(P)}}\|x(t_0)\|.\end{aligned} \tag{35}$$

Thus, $m$ need to be chosen to meet

$$m \geq r^{n}\|K\|\sqrt{\frac{\lambda_{\max}(P)}{\lambda_{\min}(P)}}\|x(t_0)\|, \tag{36}$$

which would satisfy the requirement. This ends the proof. □

The design process can be summarized as Algorithm 1:

**Algorithm 1:** Implementation of State Feedback PWM Controller.

```
/* Offline Design                                                    */
```
1 Given the matrices $A, B$ in (9), select $K^T \in \mathbb{R}^n$, and $P \in \mathbb{R}^{n\times n}$ such that (14) holds;
2 For the obtained $K$ and $P$, compute constant $\alpha_m$ in (21) and choose a suitable $r$ satisfying (32);
3 Based on the parameter $r$, choose the sampling size $T$ satisfying $rT \leq \alpha_m$;
4 For given area $\Omega$ with $x(t_0) \in \Omega$, get the amplitude $m$ satisfying (36);
```
/* Online Design                                                     */
```
5 **while** $t \in [t_k, t_{k+1})$ **do**
6  Determine $s_k, d_k$ according to (6);
7  Update the sampling index $k = k + 1$;
8 **end**

## 4. Output feedback control

### 4.1. Control design

In many scenarios, the system state is not available. In this section, we consider the design problem of output feedback control. Based on the observer design technology proposed in [38], we consider the variables as

$$\begin{aligned}&\dot{\hat{x}}(t) = A\hat{x}(t) + Bu(t), t \in [t_k, t_{k+1}),\\ &\hat{x}(t_{k+1}) = \hat{x}\left(t_{k+1}^-\right) - T\Gamma L\left(C\hat{x}\left(t_{k+1}^-\right) - y\left(t_{k+1}^-\right)\right),\end{aligned} \tag{37}$$

where

$$A=\begin{pmatrix}0&1&0&\cdots&0\\0&0&1&\cdots&0\\\vdots&\vdots&\vdots&&\vdots\\0&0&0&\cdots&1\\0&0&0&\cdots&0\end{pmatrix},\quad B=\begin{pmatrix}0\\0\\\vdots\\0\\1\end{pmatrix},\quad C=\begin{pmatrix}1&0&0&\cdots&0\end{pmatrix}. \tag{38}$$

Here, $\Gamma=\text{diag}\left\{\frac{1}{r},\frac{1}{r^2},\ldots,\frac{1}{r^n}\right\}$ where $r\geq 1$ be a parameter to be designed. Vector $L$ is the observer gain to be determined.

Then, through considering the state transformation $z(t)=\Gamma\hat{x}(t)$, we design

$$s_k=\text{sign}(Kz(t_k)),\quad d_k=\left|\frac{r^{n+1}Kz(t_k)}{m}\right|\cdot 100\%, \tag{39}$$

where vector $K$ is the control gain to be determined.

### 4.2. Stability analysis

**Theorem 2.** *Supposed that Assumption 1 is satisfied. Let vectors $K$, $L$ be designed to satisfy*

$$\begin{pmatrix}A+BK&-LC\\0&A+LC\end{pmatrix}^T P+P\begin{pmatrix}A+BK&-LC\\0&A+LC\end{pmatrix}\leq -I, \tag{40}$$

*where $P$ is a positive definite matrix.*

*For any initial state $x(t_0)\in\mathbb{R}^n$, through choosing appropriate sampling size $T$ and control parameter $r$, system (1) can be stabilized through the PWM signal (3), (6) if the PWM amplitude $m$ is sufficient large.*

**Proof.** Considering the error state $e(t)=\Gamma x(t)-z(t)$, we obtain

$$\begin{aligned}\dot{e}(t)&=rAe(t)+F(t),t\in[t_k,t_{k+1}),\\e(t_{k+1})&=(I+rTLC)e\left(t_{k+1}^-\right),\end{aligned} \tag{41}$$

where

$$F(t)=\begin{pmatrix}\frac{1}{r}f_1(x_1(t))\\\frac{1}{r^2}f_2(x_1(t),x_2(t))\\\vdots\\\frac{1}{r^{n-1}}f_{n-1}(x_1(t),x_2(t),\ldots,x_{n-1}(t))\\\frac{1}{r^n}f_n(x_1(t),x_2(t),\ldots,x_{n-1}(t),x_n(t))\end{pmatrix}. \tag{42}$$

Meanwhile, under the state transformation $z(t)=\Gamma\hat{x}(t)$, the dynamic (37) is transformed into

$$\begin{aligned}\dot{z}(t)&=rAz(t)+\frac{1}{r^n}Bu(t),t\in[t_k,t_{k+1}),\\z(t_{k+1})&=z\left(t_{k+1}^-\right)-rTLCe\left(t_{k+1}^-\right),\end{aligned} \tag{43}$$

Solving the above equations get

$$e(t_{k+1})=(I+rTLC)e^{rTA}e(t_k)+(I+rTLC)\int_{t_k}^{t_{k+1}}e^{rA(t_{k+1}-s)}F(s)ds. \tag{44}$$

and

$$z(t_{k+1}) = e^{rTA}z(t_k) + \int_{t_k}^{t_{k+1}} e^{rA(t_{k+1}-s)}\frac{1}{r^n}Bu(s)ds$$
$$-rTLC\left(e^{rTA}e(t_k) + \int_{t_k}^{t_{k+1}} e^{rA(t_{k+1}-s)}F(s)ds\right). \tag{45}$$

For the control input, we have the relation

$$\int_{t_k}^{t_{k+1}} e^{rA(t_{k+1}-s)}\frac{1}{r^n}Bu(s)ds = \int_0^{rT} e^{A(rT-s)}\frac{1}{r^{n+1}}Bu\left(t_k + \frac{s}{r}\right)ds$$
$$= \int_0^{r\delta_k} e^{A(rT-s)}BKz(t_k)ds = \int_0^{r\delta_k} e^{A(rT-s)}\frac{1}{r^{n+1}}Bms_k ds$$
$$= \frac{1}{d_k}\int_0^{rd_kT} e^{A(rT-s)}BKz(t_k)ds. \tag{46}$$

Let

$$M(\alpha,\tau) = \begin{pmatrix} e^{\alpha A} + \frac{1}{\tau}\int_0^{\tau\alpha} e^{A(\alpha-s)}BKds & -\alpha LCe^{\alpha A} \\ (I+\alpha LC)e^{\alpha A} \end{pmatrix} \tag{47}$$

be a matrix function defined on $[0,1]\times(0,1]$. From (44) and (45), we get the closed-loop system as

$$Z(t_{k+1}) = M(rT,d_k)z(t_k) + \tilde{F}(t_k), \tag{48}$$

where $Z(t) = \left(z^T(t), e^T(t)\right)^T$, and

$$\tilde{F}(t_k) = \begin{pmatrix} -rTLC\int_{t_k}^{t_{k+1}} e^{rA(t_{k+1}-s)}F(s)ds \\ (I+rTLC)\int_{t_k}^{t_{k+1}} e^{rA(t_{k+1}-s)}F(s)ds \end{pmatrix} \tag{49}$$

Let the Lyapunov function be $V_k = Z^T(t_k)PZ(t_k)$.

Then, it holds

$$V_{k+1} = \left(M(rT,d_k)Z(t_k) + \tilde{F}(t_k)\right)^T P\left(M(rT,d_k)Z(t_k) + \tilde{F}(t_k)\right)$$
$$= Z^T(t_k)M^T(rT,d_k)PM(rT,d_k)Z(t_k) + 2Z^T(t_k)M^T(rT,d_k)P\tilde{F}(t_k)$$
$$+\tilde{F}^T(t_k)P\tilde{F}(t_k). \tag{50}$$

To continue, we need to analyze the matrix function $M(\alpha,\tau)$ and the nonlinear function $\tilde{F}(t_k)$. A similar analysis with the state feedback case can also get a positive constant $\alpha_m$ such that

$$M^T(\alpha,\tau)PM(\alpha,\tau) \le P - \frac{\alpha}{2}I, \quad \alpha\in[0,\alpha_m], \quad \tau\in[0,1]. \tag{51}$$

Back to (50), we turn to estimate the nonlinear term $\tilde{F}(t_k)$. Under Assumption 1, we get, for $i = 1,2,\ldots,n$,

$$\frac{1}{r^i}|f_i(x_1,x_2,\ldots,x_i)| \le \theta\left(\left|\frac{1}{r}x_1\right| + \left|\frac{1}{r^2}x_2\right| + \ldots + \left|\frac{1}{r^i}x_i\right|\right) \le \theta\sqrt{n}(\|z\| + \|e\|), \tag{52}$$

which further yields

$$\|F(t)\| \le \theta n(\|z\| + \|e\|). \tag{53}$$

Meanwhile, one obtains

$$\frac{d}{dt}\|e(t)\| \le \|\dot{e}(t)\| \le r\|A\|\|e(t)\| + \theta n(\|z\| + \|e\|), \tag{54}$$

and

$$\frac{d}{dt}\|z(t)\| \le \|\dot{z}(t)\| \le r\|A\|\|z(t)\| + \frac{1}{r^n}\|B\||u(t)|. \tag{55}$$

It holds

$$\int_{t_k}^{t_k+d_k} |u(s)|ds = |rKz(t_k)| \le r\|K\|\|z(t_k)\|. \tag{56}$$

In (54), integrating the left part from $t_k$ to $t$ $(t \in [t_k, t_{k+1}))$, one gets

$$\|e(t)\| \le \|e(t_k)\| + (r\|A\| + \theta n)\int_{t_k}^{t} \|e(s)\|ds + \theta n\int_{t_k}^{t} \|z(s)\|ds, \tag{57}$$

and

$$\|z(t)\| \le \|z(t_k)\| + r\|A\|\int_{t_k}^{t} \|z(s)\|ds + \|B\|\|K\|\|z(t_k)\|. \tag{58}$$

Then, it holds

$$\begin{aligned}\|z(t)\| + \|e(t)\| \le{}& (1 + \|B\|\|K\|)(\|z(t_k)\| + \|e(t_k)\|)\\ &+(r\|A\| + \theta n)\int_{t_k}^{t} (\|z(t)\| + \|e(t)\|)ds.\end{aligned} \tag{59}$$

Then, using the Grönwall's inequality, one obtains

$$\begin{aligned}\|z(t)\| + \|e(t)\| &\le (1 + \|B\|\|K\|)e^{(r\|A\|+\theta n)(t-t_k)}(\|z(t_k)\| + \|e(t_k)\|)\\ &\le \sqrt{2}(1 + \|B\|\|K\|)e^{(r\|A\|+\theta n)(t-t_k)}\|Z(t_k)\|.\end{aligned} \tag{60}$$

In this case, the nonlinear term $\int_{t_k}^{t_{k+1}} e^{rA(t_{k+1}-s)}F(s)ds$ is estimated as below:

$$\begin{aligned}&\left\|\int_{t_k}^{t_{k+1}} e^{rA(t_{k+1}-s)}F(s)ds\right\|\\ &\le \int_{t_k}^{t_{k+1}} e^{r\|A\|(t_{k+1}-s)}\|F(s)\|ds\\ &\le \int_{t_k}^{t_{k+1}} \theta n e^{r\|A\|(t_{k+1}-s)}\sqrt{2}(1 + \|B\|\|K\|)e^{(r\|A\|+\theta n)(s-t_k)}\|Z(t_k)\|ds\\ &\le \int_{t_k}^{t_{k+1}} \theta n e^{rT\|A\|}\sqrt{2}(1 + \|B\|\|K\|)e^{\theta n(s-t_k)}\|Z(t_k)\|ds\\ &\le e^{\|A\|}\sqrt{2}(1 + \|B\|\|K\|)\left(e^{\theta nT} - 1\right)\|Z(t_k)\|.\end{aligned} \tag{61}$$

which further yields

$$\tilde{F}(t_k) = \begin{pmatrix} -rTLC\int_{t_k}^{t_{k+1}} e^{rA(t_{k+1}-s)}F(s)ds \\ (I + rTLC)\int_{t_k}^{t_{k+1}} e^{rA(t_{k+1}-s)}F(s)ds \end{pmatrix} \tag{62}$$

$$\left\|\tilde{F}(t_k)\right\| \le 2(1 + \|LC\|)e^{\|A\|}(1 + \|B\|\|K\|)\left(e^{\theta nT} - 1\right)\|Z(t_k)\| \tag{63}$$

Thus, back to (50), we get that, when $rT \le \alpha_m$, it holds

$$\begin{aligned} V_{k+1} &\le V_k - \frac{rT}{2}\|Z(t_k)\|^2 + 2Z^T(t_k)M^T(rT, d_k)P\tilde{F}(t_k) + \tilde{F}^T(t_k)P\tilde{F}(t_k) \\ &\le V_k - \frac{rT}{2}\|Z(t_k)\|^2 + 4\varpi\|P\|(1+\|LC\|)e^{\|A\|}(1+\|B\|\|K\|)\left(e^{\theta nT}-1\right)\|Z(t_k)\|^2 \\ &\quad +4\|P\|(1+\|LC\|)^2(1+\|B\|\|K\|)^2e^{2\|A\|}\left(e^{\theta nT}-1\right)^2\|Z(t_k)\|, \end{aligned} \tag{64}$$

where $\varpi$ is the upper bounded of $\|M(\alpha,\tau)\|$ on the area $[0,1]\times(0,1]$.

When $T \in (0,1]$, it holds $e^{\theta nT}-1 \le T\left(e^{\theta n}-1\right)$. Thus, when

$$\begin{aligned} r \ge\ & 16\varpi\|P\|(1+\|LC\|)(1+\|B\|\|K\|)e^{\|A\|}\left(e^{\theta n}-1\right) \\ & +16\|P\|(1+\|LC\|)^2(1+\|B\|\|K\|)^2e^{2\|A\|}\left(e^{\theta n}-1\right)^2, \end{aligned} \tag{65}$$

we get

$$V_{k+1} \le V_k - \frac{rT}{4}\|z(t_k)\|^2. \tag{66}$$

Therefore, the convergence of $V_k$ is ensured. Since $r$ is a constant, it is achieved that system (1) under PWM control (3), (39) is stable at equilibrium point $x=0$, $\hat{x}=0$.

The choosing of $m$ is depended on both the initial system state $x(0)$ and the initial observer state $\hat{x}(0)$. In detail, it is needed that $m \ge |r^{n+1}Kz(t_k)|$ for any index $k$. Since $V_{k+1} \le V_k \le \ldots \le V_0$ we get

$$\begin{aligned} &\left|r^{n+1}Kz(t_k)\right| \le r^{n+1}\|K\|\|z(t_k)\| \le r^{n+1}\|K\|\sqrt{\frac{V_k}{\lambda_{\min}(P)}} \le r^{n+1}\|K\|\sqrt{\frac{V_0}{\lambda_{\min}(P)}} \\ &\le r^{n+1}\|K\|\sqrt{\frac{\lambda_{\max}(P)}{\lambda_{\min}(P)}}\max\left\{\|z(t_0)\|, \|e(t_0)\|\right\} \\ &\le 2r^n\|K\|\sqrt{\frac{\lambda_{\max}(P)}{\lambda_{\min}(P)}}\max\left\{\|x(t_0)\|, \left\|\hat{x}(t_0)\right\|\right\} \end{aligned} \tag{67}$$

Thus, $m$ need to be chosen to meet

$$m \ge 2r^n\|K\|\sqrt{\frac{\lambda_{\max}(P)}{\lambda_{\min}(P)}}\max\left\{\|x(t_0)\|, \left\|\hat{x}(t_0)\right\|\right\}, \tag{68}$$

which would satisfy the requirement.

This ends the proof. □

The design process can be summarized as Algorithm 2:

**Remark 2.** Our design is mainly based on the high gain feedback control method. First, we consider a state transformation to get a new variable $z(t)$ which involves a parameter $r$ to be determined. Then, we compute the variables $s_k$, $d_k$ in PWM signal based on the new variable $z(t)$. At last, based on the Lyapunov analysis, we determine the parameter $r$ and sampling size $T$ to ensure the system convergence.

**Remark 3.** Noticed that the main contribution in this paper is to design the stabilizing controller for a strict-feedback nonlinear system via the PWM signal. The introduced method is based on the high gain control method, and there are some limitations, such as the high amplitude $m$, the small sampling size $T$, and the frequent switching. Because the strict-feedback

**Algorithm 2:** Implementation of Output Feedback PWM Controller.

/* Offline Design */

Given the matrices $A, B, C$ in (38), select $K^T \in \mathbb{R}^n$, $L \in \mathbb{R}$ and $P \in \mathbb{R}^{2n\times 2n}$ such that (40) holds;

For the obtained $K, L$ and $P$, compute constant $\alpha_m$ in (51) and choose a suitable $r$ satisfying (65);

Based on the parameter $r$, choose the sampling size $T$ satisfying $rT \le \alpha_m$;

For given area $\Omega$ with $x(t_0), \hat{x}(t_0) \in \Omega$, get the amplitude $m$ satisfying (68);

/* Online Design */

**while** $t \in [t_k, t_{k+1})$ **do**

  **if** $k \neq 0$ **then**

    Update the state $\hat{x}(t_k)$ through (37);

  **end**

  Determine $s_k, d_k$ according to (39);

  Update the sampling index $k = k + 1$;

**end**

nonlinear system is high-order and nonlinear. To dominate such a system, a high amplitude $m$ and a small sampling size $T$ may be demanded. The high amplitude $m$ results in spike phenomena in the system performance, since the state $z(t)$ ranges in a large area. Meanwhile, due to small sampling size $T$, the undesired high frequent would also happen. On the one hand, we may introduce too many inequalities in the analysis process. In most scenarios, the convergence is still achieved, even choosing a large sampling size $T$ and a small parameter $r$. On the other hand, we provide a relation about these parameters, and we can comprehensively consider all these parameters to get the stabilizing controller. For example, if the initial state is smaller, one can choose a small amplitude $m$.

## 5. Simulation examples

**Example 1.** Consider the nonlinear system

$$\dot{x}_1(t) = x_2(t) + \sin(x_1(t))x_1(t), \quad \dot{x}_2(t) = u(t), \tag{69}$$

where $x = (x_1, x_2)^T$ is the system state, $u$ is the system input. The measurement is $x(kT)$ in the state feedback case, and $y(kT) = x_1(kT)$ in the output feedback case, where $T > 0$ is the sampling size, and $k$ is the index. Obviously, the nonlinearity $\sin(x_1)x_1$ satisfies Assumption 1 with $\theta = 1$.

I. *The State Feedback Case:* The PWM control $u(t)$ is described as

$$u(t) = \begin{cases} ms_k, & t \in [kT,\ kT + \delta_k), \\ 0, & t \in [kT + \delta_k,\ (k+1)T), \end{cases} \tag{70}$$

where variables $s_k$, $\delta_k$ are designed as

$$\begin{aligned} s_k &= \operatorname{sign}\big(k_1 r^2 x_1(kT) + k_2 r x_2(kT)\big), \\ \delta_k &= T \cdot \left| \tfrac{k_1 r^2 x_1(kT) + k_2 r x_2(kT)}{m} \right| \cdot 100\%. \end{aligned} \tag{71}$$

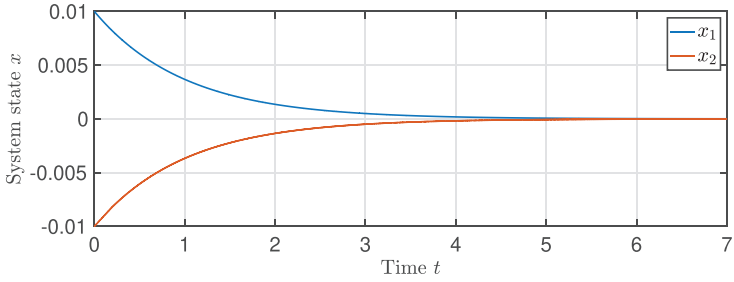


(a) The trajectory of state $x_1(t)$, $x_2(t)$.

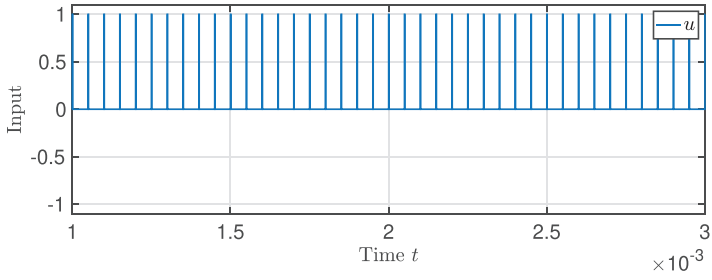


(b) The trajectory of input $u(t)$.

Fig. 1. Trajectory of system (69) under control (70),(71).

Let $m = 1$, $T = 0.00005$, $r = 2$, $k_1 = -1$ and $k_2 = -2$. The trajectory of system (69) under PWM control (70), (71) is shown in Fig. 1. It can be seen from Fig. 1a that the state trajectories are converging to zero, and the control signal in Fig. 1b is in pulse form. This illustrates the effectiveness of our design method.

II. *The Output Feedback Case:* For the output case, the auxiliary variables $\hat{x}_1$, $\hat{x}_2$ are designed as

$$\begin{aligned}
&\dot{\hat{x}}_1(t) = \hat{x}_2(t), \quad \dot{\hat{x}}_2(t) = u(t), \quad t \in [t_k, t_{k+1}),\\
&\hat{x}_1(t_{k+1}) = \hat{x}_1(t_{k+1}^-) + l_1 \tfrac{T}{r}(\hat{x}_1(t_{k+1}^-) - y(t_{k+1})),\\
&\hat{x}_2(t_{k+1}) = \hat{x}_2(t_{k+1}^-) + l_2 \tfrac{T}{r^2}(\hat{x}_1(t_{k+1}^-) - y(t_{k+1})),
\end{aligned} \tag{72}$$

where $t_k = kT$. Then, based on the variables $\hat{x}_1(t)$ and $\hat{x}_2(t)$, we design the PWM control as

$$u(t) = \begin{cases} ms_k, & t \in [kT,\ kT + \delta_k),\\ 0, & t \in [kT + \delta_k,\ (k+1)T), \end{cases} \tag{73}$$

where

$$\begin{aligned}
&s_k = \operatorname{sign}\big(k_1 r^2 \hat{x}_1(kT) + k_2 r \hat{x}_2(kT)\big),\\
&\delta_k = T \cdot \left| \frac{k_1 r^2 \hat{x}_1(kT) + k_2 r \hat{x}_2(kT)}{m} \right| \cdot 100\%.
\end{aligned} \tag{74}$$

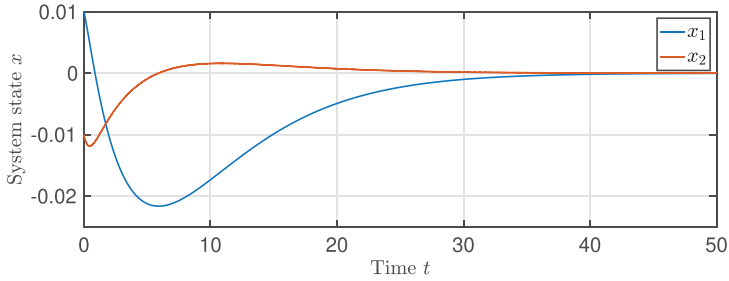


(a) The trajectory of states $x_1(t)$ and $x_2(t)$.

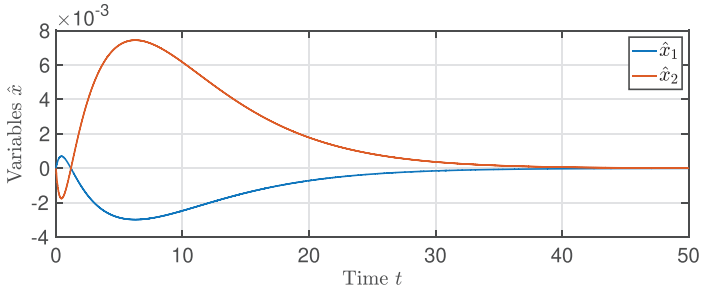


(b) The trajectory of variables $\hat{x}_1(t)$ and $\hat{x}_2(t)$.

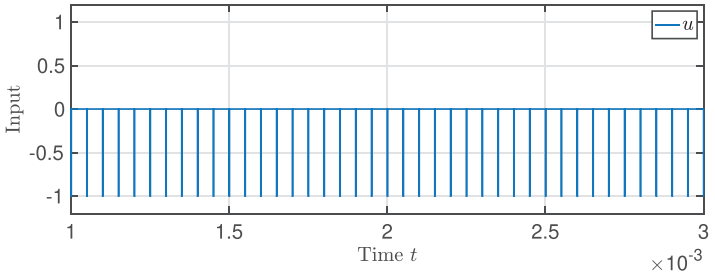


(c) The trajectory of input $u(t)$

Fig. 2. Trajectory of system (69) under control (73), (74).

Let $r = 5$, $T = 0.00005$, $m = 5$, $l_1 = -2$, $l_2 = -1$, $k_1 = -2$ and $k_2 = -1$. The system trajectory is shown in Fig. 2. It can be seen in Fig. 2c that the control input is in PWM form. One can also seen in Fig. 2a that the system states $x_1(t)$, $x_2(t)$ converge to the equilibrium point $x = 0$, and in Fig. 2b that the variables $\hat{x}_1(t)$, $\hat{x}_2(t)$ converge to the equilibrium point $\hat{x} = 0$. This verifies the effectiveness of Theorem 2.

**Example 2.** Consider an electromechanical system, which is shown in Fig. 3.

Following the result in [40], we describe the dynamic as

$$\begin{aligned} &M\ddot{q} + B\dot{q} + N\sin(q) = I, \\ &L\dot{I} = V_0 - RI - K_B\dot{q}, \end{aligned} \tag{75}$$

where $M = \frac{J}{K_\tau} + \frac{mL_0^2}{3K_\tau} + \frac{M_0L_0^2}{K_\tau} + \frac{2M_0R_0^2}{5K_\tau}$, $N = \frac{mL_0G}{2K_\tau} + \frac{M_0L_0G}{K_\tau}$, and $B = \frac{B_0}{K_\tau}$. $J$ is the rotor inertia, $m$ is the link mass, $M_0$ is the load mass, $L_0$ is the link length, $R_0$ is the radius of the load, $G$ is

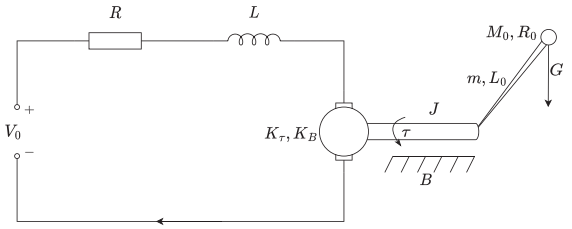


Fig. 3. Schematic of the electromechanical system.

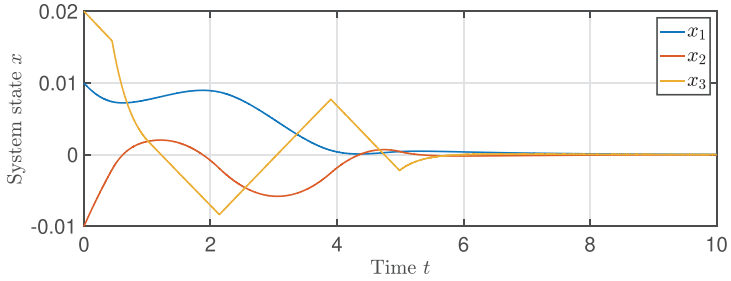


Fig. 4. The trajectory of state $x_1(t)$, $x_2(t)$ and $x_3(t)$ in system (76) under control (77),(78).

the gravity coefficient, $B_0$ is the coefficient of viscous friction at the joint, $q(t)$ is the angular motor position (and, hence, the position of the load), $I(t)$ is the motor armature current, and $K_\tau$ is the coefficient that characterizes the electromechanical conversion of armature current to torque. $L$ is the armature inductance, $R$ is the armature resistance, $K_B$ is the back EMF coefficient, and $V_0$ is the input control voltage. The values of the parameters are chosen as $J = 162.5kg \cdot m^2$, $m = 0.506kg$, $R_0 = 0.023m$, $M_0 = 0.434kg$, $L_0 = 0.305m$, $B_0 = 16.25 \times 10^{-3}N \cdot m \cdot s/rad$, $L = 50H$, $R = 0.05\Omega$, and $K_\tau = K_B = 0.90N \cdot m/A$.

We also consider the variables $x_1 = q$, $x_2 = \dot{q}$, $x_3 = \frac{I}{M}$, and $u = \frac{V_0}{ML}$. Then, the dynamic can be written as

$$\begin{aligned}
\dot{x}_1 &= x_2,\\
\dot{x}_2 &= x_3 - \frac{N}{M}\sin x_1 - \frac{B}{M}x_2,\\
\dot{x}_3 &= u - \frac{K_B}{ML}x_2 - \frac{R}{L}x_3.
\end{aligned} \tag{76}$$

Obviously, system (76) is in the strict-feedback nonlinear system, and $f_1 = 0$, $f_2(x_1, x_2) = -\frac{N}{M}\sin x_1 - \frac{B}{M}x_2$, $f_3(x_1, x_2, x_3) = -\frac{K_B}{ML}x_2 - \frac{R}{L}x_3$.

I. *The State Feedback Case:* The PWM control $u(t)$ is described by

$$u(t) = \begin{cases} ms_k, & t \in [kT,\ kT + \delta_k),\\ 0, & t \in [kT + \delta_k,\ (k+1)T), \end{cases} \tag{77}$$

where the variables $s_k$, $\delta_k$ are designed as

$$\begin{aligned}
s_k &= \operatorname{sign}\big(k_1 r^3 x_1(kT) + k_2 r^2 x_2 + k_3 r x_3(kT)\big),\\
\delta_k &= T \cdot \left| \frac{k_1 r^3 x_1(kT) + k_2 r^2 x_2 + k_3 r x_3(kT)}{m} \right| \cdot 100\%.
\end{aligned} \tag{78}$$

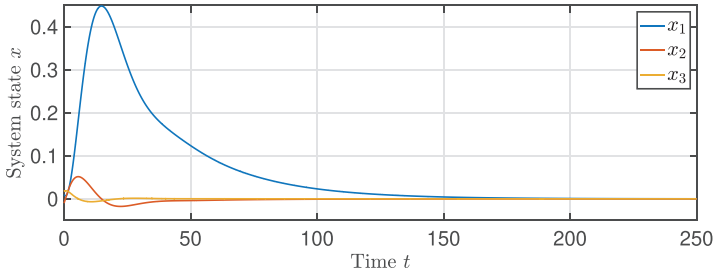


(a) The trajectory of states $x_1(t)$, $x_2(t)$ and $x_3(t)$.

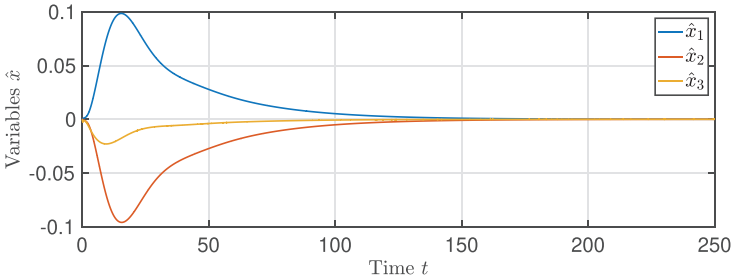


(b) The trajectory of variables $\hat{x}_1(t)$, $\hat{x}_2(t)$ and $\hat{x}_3(t)$.

Fig. 5. Trajectory of system (76) under control (80), (81).

Let $m = 1$, $T = 0.00001$, $r = 2$, $k_1 = -0.3$ and $k_2 = -1.2$, and $k_3 = -0.7$. The trajectory of system (76) under PWM control (77), (78) is shown in Fig. 4. It can be seen that all the state $x_1, x_2, x_3$ are converging to zero. This illustrates the effectiveness of our design method.

II. *The Output Feedback Case:* For the output case, the auxiliary variables $\hat{x}_1$, $\hat{x}_2$, $\hat{x}_3$ are designed as

$$\begin{aligned}
&\dot{\hat{x}}_1(t) = \hat{x}_2(t), \quad \dot{\hat{x}}_2(t) = \hat{x}_3(t), \quad \dot{\hat{x}}_3(t) = u(t), \quad t \in [t_k, t_{k+1}),\\
&\hat{x}_1(t_{k+1}) = \hat{x}_1(t_{k+1}^-) + l_1 \tfrac{T}{r}(\hat{x}_1(t_{k+1}^-) - y(t_{k+1})),\\
&\hat{x}_2(t_{k+1}) = \hat{x}_2(t_{k+1}^-) + l_2 \tfrac{T}{r^2}(\hat{x}_1(t_{k+1}^-) - y(t_{k+1})),\\
&\hat{x}_3(t_{k+1}) = \hat{x}_3(t_{k+1}^-) + l_3 \tfrac{T}{r^3}(\hat{x}_1(t_{k+1}^-) - y(t_{k+1})),
\end{aligned} \tag{79}$$

where $t_k = kT$. Then, based on the variables $\hat{x}_1(t)$, $\hat{x}_2(t)$ and $\hat{x}_3(t)$, we design the PWM control as (Algorithms 1 and 2)

$$u(t) = \begin{cases} ms_k, & t \in [kT,\ kT + \delta_k),\\ 0, & t \in [kT + \delta_k,\ (k+1)T), \end{cases} \tag{80}$$

where the variables $s_k$, $\delta_k$ are

$$\begin{aligned}
&s_k = \operatorname{sign}\big(k_1 r^3 \hat{x}_1(kT) + k_2 r^2 \hat{x}_2(kT) + k_3 r \hat{x}_3(kT)\big),\\
&\delta_k = T \cdot \left| \tfrac{k_1 r^3 \hat{x}_1(kT) + k_2 r^2 \hat{x}_2(kT) + k_3 r \hat{x}_3(kT)}{m} \right| \cdot 100\%.
\end{aligned} \tag{81}$$

Let $r = 4$, $T = 0.00001$, $m = 1$, $l_1 = -1.1$, $l_2 = -1.2$, $l_3 = -0.7$, $k_1 = -0.3$, $k_2 = -1.2$ and $k_3 = -0.7$. The system trajectory is shown in Fig. 5. One can see in Fig. 5a that the system states $x_1(t)$, $x_2(t)$ and $x_3(t)$ converge to the equilibrium point $x = 0$, and in Fig. 5b

that the variables $\hat{x}_1(t)$, $\hat{x}_2(t)$ and $\hat{x}_3(t)$ also converge to the equilibrium point $\hat{x} = 0$. This verifies the effectiveness of Theorem 2.

## 6. Conclusion

This paper proposed a novel method to design the PWM control. Considering the discontinuous character of a PWM signal, we analyzed the switching performance of the system dynamics. Through modelling the pulse width as a parameter, both the state feedback case and the output feedback case were considered. It was proved that under a certain condition on the PWM amplitude and sampling size, the asymptotic convergence could be achieved for a class of strict-feedback nonlinear systems. Two examples were given to illustrate the effectiveness of our proposed method. In the future, the following aspects can be further investigated: 1, the PWM control can be designed to cope with the system disturbance, and the robustness analysis can be studied; 2, the PWM control can be studied for more complex nonlinear systems involving other factors such as delays, uncertain coefficients, uncertain nonlinearities.

## Declaration of Competing Interest

The authors declare that they have no known competing financial interests or personal relationships that could have appeared to influence the work reported in this paper.

## CRediT authorship contribution statement

**Le Chang:** Conceptualization, Methodology, Investigation, Writing – original draft, Writing – review & editing. **Xiaowei Shao:** Supervision, Investigation, Project administration, Writing – review & editing. **Dexin Zhang:** Resources, Investigation, Writing – review & editing.

## References

[1] R.C. Dorf, R.H. Bishop, Modern control systems, Pearson Prentice Hall, 2008.
[2] G.N. Nair, Quantized Control and Data Rate Constraints, in: Encyclopedia of systems and control, Springer, 2021, pp. 1794–1800.
[3] A. Isidori, Nonlinear control systems: An introduction, Springer, 1985.
[4] H.K. Khalil, Nonlinear control, Pearson New York, 2015.
[5] J. Zhou, C. Wen, Adaptive backstepping control of uncertain systems, Springer, Berlin Heidelberg, 2008.
[6] M.M. Zirkohi, T. Kumbasar, Adaptive backstepping controller design for mimo cancer immunotherapy using laguerre polynomials, J. Franklin Inst. 357 (8) (2020) 4664–4679.
[7] K. He, C. Dong, Q. Wang, Anti-disturbance dynamic inversion backstepping control for uncertain pure-feedback systems via multiple extended state observers, J. Franklin Inst. 358 (13) (2021) 6385–6407.
[8] X. Yu, X. Meng, X. Zheng, Y. Liu, Improved adaptive backstepping control of MPCVD reactor systems with non-parametric uncertainties, J. Franklin Inst.. (In Press). doi:10.1016/j.jfranklin.2022.09.052.
[9] W. Liu, X. Cheng, J. Zhang, Command filter-based adaptive fuzzy integral backstepping control for quadrotor uav with input saturation, J. Franklin Inst.. (In Press). doi:10.1016/j.jfranklin.2022.10.042.
[10] Z. Qin, T. Liu, Z.P. Jiang, Adaptive backstepping for distributed optimization, Automatica 141 (2022). Article No. 110304
[11] M.-S. Koo, H.-L. Choi, J.T. Lim, Global regulation of a class of uncertain nonlinear systems by switching adaptive controller, IEEE Trans Automat Contr 55 (12) (2010) 2822–2827.
[12] X. Zhang, L. Liu, G. Feng, C. Zhang, Output feedback control of large-scale nonlinear time-delay systems in lower triangular form, Automatica 49 (11) (2013) 3476–3483.
[13] X. Chen, X. Zhang, C. Zhang, L. Chang, Global asymptotic stabilization for input-delay chained nonholonomic systems via the static gain approach, J. Franklin Inst. 355 (9) (2018) 3895–3910.

[14] L. Fu, R. Ma, H. Pang, J. Fu, Predefined-time tracking of nonlinear strict-feedback systems with time-varying output constraints, J. Franklin Inst. 359 (8) (2022) 3492–3516.
[15] X. Yuan, B. Chen, C. Lin, Fuzzy adaptive output-feedback tracking control for nonlinear strict-feedback systems in prescribed finite time, J. Franklin Inst. 358 (15) (2021) 7309–7332.
[16] X. Deng, C. Zhang, Y. Ge, Adaptive neural network dynamic surface control of uncertain strict-feedback nonlinear systems with unknown control direction and unknown actuator fault, J. Franklin Inst. 359 (9) (2022) 4054–4073.
[17] Z. Yang, X. Zhang, X. Zong, G. Wang, Adaptive fuzzy control for non-strict feedback nonlinear systems with input delay and full state constraints, J. Franklin Inst. 357 (11) (2020) 6858–6881.
[18] C. Qian, H. Du, Global output feedback stabilization of a class of nonlinear systems via linear sampled-data control, IEEE Trans. Automat. Contr. 57 (11) (2012) 2934–2939.
[19] H.-Y. Guo, X.G. Zhang, Sampled observer-based adaptive decentralized control for strict-feedback interconnected nonlinear systems, J. Franklin Inst. 358 (11) (2021) 5845–5861.
[20] H. Li, Q. Liu, X. Zhang, X. Chen, Quantized control for the class of feedforward nonlinear systems, Science China Information Sciences 62 (8) (2019).
[21] Z.-P. Jiang, T.F. Liu, Quantized nonlinear control–a survey, Acta Autom. Sin. 39 (11) (2013) 1820–1830.
[22] C. Zheng, L. Li, L. Wang, C. Li, How much information is needed in quantized nonlinear control? Sci. China Informa. Sci. 61 (9) (2018) 1–13.
[23] Y.H. Choi, S.J. Yoo, Neural-networks-based adaptive quantized feedback tracking of uncertain nonlinear strict-feedback systems with unknown time delays, J. Franklin Inst. 357 (15) (2020) 10691–10715.
[24] A. Komaee, Stabilization of linear systems by pulsewidth modulation of switching actuators, IEEE Trans. Automat. Contr. 65 (5) (2020) 1969–1984.
[25] L. Hou, A.N. Michel, Stability analysis of pulse-width-modulated feedback systems, Automatica 37 (9) (2001) 1335–1349.
[26] T. Kadota, H. Bourne, Stability conditions of pulse-width-modulated systems through the second method of Lyapunov, IRE Trans. Autom. Control 6 (3) (1961) 266–276.
[27] T. Liu, Z.P. Jiang, Distributed control of multi-agent systems with pulse-width-modulated controllers, Automatica 119 (2020). Article No. 109020
[28] S.-L. Jung, Y.Y. Tzou, Discrete sliding-mode control of a PWM inverter for sinusoidal output waveform synthesis with optimal sliding curve, IEEE Trans. Power Electron. 11 (4) (1996) 567–577.
[29] E.-C. Chang, Y.-C. Liu, C.H. Chang, Experimental performance comparison of various sliding modes controlled PWM inverters, Energy Procedia 156 (2019) 110–114.
[30] A.G. Beccuti, G. Papafotiou, M. Morari, et al., Hybrid Control Techniques for Switched-mode DC-DC Converters Part II: The Step-up Topology, in: 2007 American Control Conference, IEEE, 2007, pp. 5464–5471.
[31] S. Mariethoz, S. Almer, M. Baja, et al., Comparison of hybrid control techniques for buck and boost DC-DC converters, IEEE Trans. Control Syst. Technol. 18 (5) (2010) 1126–1145.
[32] H. Fujioka, C.-Y. Kao, S. Almér, U. Jönsson, LQ optimal control for a class of pulse width modulated systems, Automatica 43 (6) (2007) 1009–1020.
[33] W.L.D. Koning, Digital optimal reduced-order control of pulse-width-modulated switched linear systems, Automatica 39 (11) (2003) 1997–2003.
[34] H. Li, X. Zhang, L. Xie, S. Liu, Q. Liu, Event-triggered tracking control for a class of nonlinear systems: a dynamic gain approach, IEEE Trans. Automat. Contr.. (Early Access). doi:10.1109/TAC.2023.3247457.
[35] J. Wu, W. Sun, S.-F. Su, Y. Wu, Adaptive asymptotic tracking control for input-quantized nonlinear systems with multiple unknown control directions, IEEE Trans. Cybern.. (Early Access). doi:10.1109/TCYB.2022.3184492.
[36] Y.H. Choi, S.J. Yoo, Quantized feedback adaptive command filtered backstepping control for a class of uncertain nonlinear strict-feedback systems, Nonlinear Dyn 99 (4) (2020) 2907–2918.
[37] V. Andrieu, M. Nadri, Observer Design for Lipschitz Systems with Discrete-time Measurements, in: 49th IEEE Conference on Decision and Control (CDC), IEEE, 2010, pp. 6522–6527.
[38] V. Andrieu, M. Nadri, U. Serres, J.C. Vivalda, Self-triggered continuous-discrete observer with updated sampling period, Automatica 62 (2015) 106–113.
[39] J. Peralez, V. Andrieu, M. Nadri, U. Serres, Event-triggered output feedback stabilization via dynamic high-gain scaling, IEEE Trans. Automat. Contr. 63 (8) (2018) 2537–2549.
[40] Y. Li, S. Tong, Y. Liu, T. Li, Adaptive fuzzy robust output feedback control of nonlinear systems with unknown dead zones based on a small-gain approach, IEEE Trans. Fuzzy Syst. 22 (1) (2014) 164–176.